

# Performance Study of Vibrating-Wire Magnet Alignment Technique

K. Fukami<sup>#</sup>, N. Azumi, S. Inoue, T. Kai, H. Kimura, J. Kiuchi, S. Matsui,  
S. Takano, T. Watanabe, and C. Zhang  
RIKEN SPring-8 Center, JASRI, SPring-8 Service Co., Ltd.

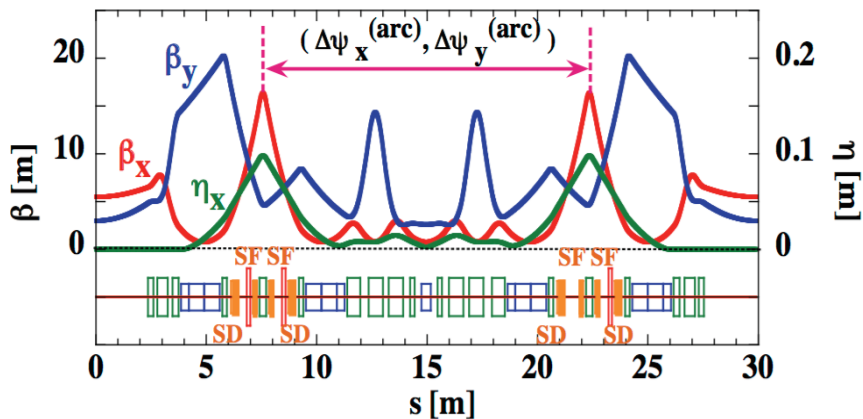
1. Introduction
2. Vibrating-Wire Technique
  - 2-1. Wire Sag
  - 2-2. Demonstration of On-Girder Alignment
  - 2-3. Overall Random Error
  - 2-4. Change in the Magnetic Center (Transport and Reassembly)
  - 2-5. Fiducialization
3. Summary

# 1. Introduction (Overview of SPring-8-II)



## SPring-8 storage ring major upgrade "SPring-8-II"

5-bend achromat, 48 cells



H. Tanaka *et al.*, "SPring-8 Upgrade Project", IPAC2016.

	SPring-8-II	SPring-8
Energy (GeV)	6	8
Stored current (mA)	>100	100
Circumference (m)	1435.45	1435.95
Effect. emittance (nmrad)	0.157 ~0.10 w/ ID	2.8

# 1. Introduction (Overview of SPring-8-II)

## 3 key developments for the SPring-8-II magnet system

1. Electromagnets based multipole magnets [1]  
High field gradient, compact, stable -> Feasible by existing technology
2. Permanent magnet based bending magnets -> Under development [2]

### 3. Precise alignment [3]

Critical for keeping enough dynamic apertures -> Today's talk

Magnet	Max. field	#/ring		cf. SPring-8
Normal bend (NB)	0.95 T	44	220	88
Longitudinal gradient bend (LGB)	0.86 T	176		
Quadrupole	56 T/m	924		470
Sextupole	2,700 T/m <sup>2</sup>	352		288

May change later.

[1] K. Fukami *et al.*, Proc. of IPAC2019, Melbourne, Australia, 2019.

[2] T. Watanabe *et al.*, Physical Review Accelerator and Beams, 20, 072401 (2017).

[3] K. Fukami *et al.*, Review of Scientific Instruments, 90, 054703 (2019).

# 1. Introduction (Magnet Alignment for SPring-8-II)

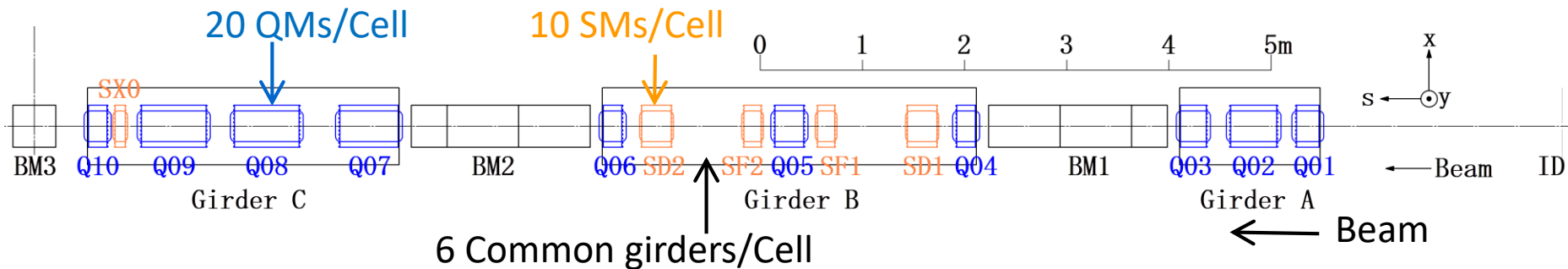
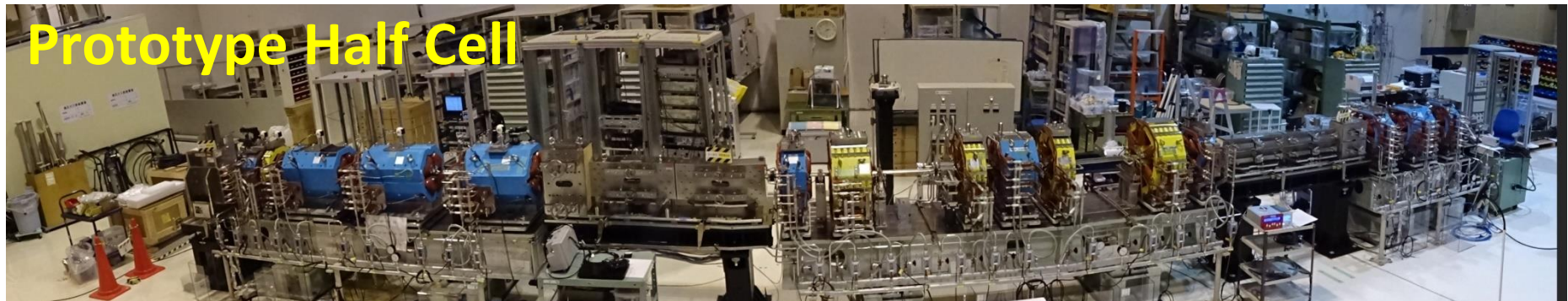
## Alignment Tolerance

On-Girder (Straight Section) :  $\Delta x, \Delta y < 25[\mu\text{m}](1\sigma)$ , Cut-off  $\pm 2\sigma$

**Our Goal** :  $\Delta x, \Delta y < 15[\mu\text{m}](1\sigma)$

Girder-to-Girder :  $\Delta x, \Delta y < 45[\mu\text{m}](1\sigma)$ , Cut-off  $\pm 2\sigma$

### Prototype Half Cell



**Need to align 1000+ $\alpha$  magnets along 1.4[km] in a year !**

## Alignment Procedure

(1) On-girder Alignment by using a Vibrating-Wire Technique out of the tunnel.

Wire sag and local kinks may increase systematic and random errors.

(2) Girder Transport into the Accelerator Tunnel.

It is necessary to evaluate a change in the magnetic center.

(3) Girder-to-Girder Alignment by using a Laser Tracker.

(4) Reassembly of Magnets to Install Vacuum Chambers.

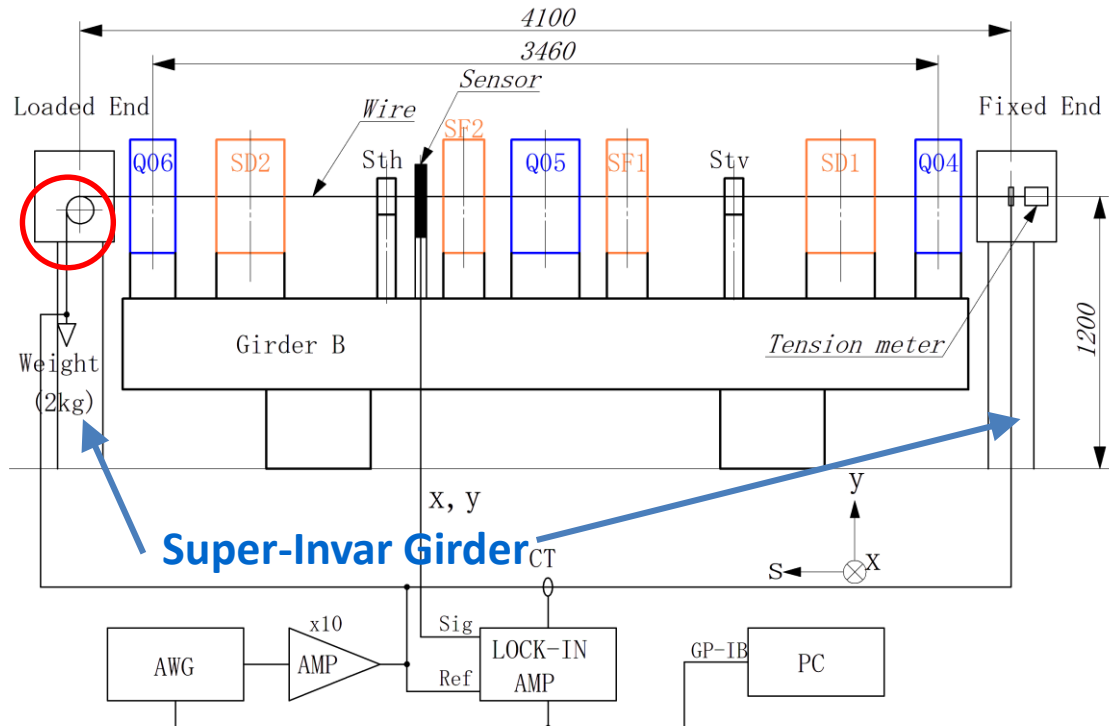
It is necessary to evaluate a change in the magnetic center.

(5) Monitoring of the Magnet Position.

We have developed a Wire Alignment Monitoring System [1].

## 2. VW Technique (Principle)

When a tensioned wire is excited with its resonance frequency, the wire vibrates. The wire in Q/S magnets does not vibrate at the position of the magnetic center. -> We can find out the magnetic center [1,2].



Wire :  
 NGK Ltd., C1720W-EHM  
 Be-Cu, 0.2[mm] $\phi$

Tension :  
 $T = 2.0$  [kgf]  
 Resonance :  
 $f_1 = 33.3$  [Hz]

Setup of the on-girder alignment for the *Girder B*. The wire was scanned using x-y stages. For the *Girder A* and *Girder C*, the setup is the same.

[1] A. Temnykh, NIM A399, 185 (1997).

[2] A. Jain *et al.*, Proc. of IWAA2008, Tsukuba, Japan, 2008.

## 2. VW Technique (Principle)

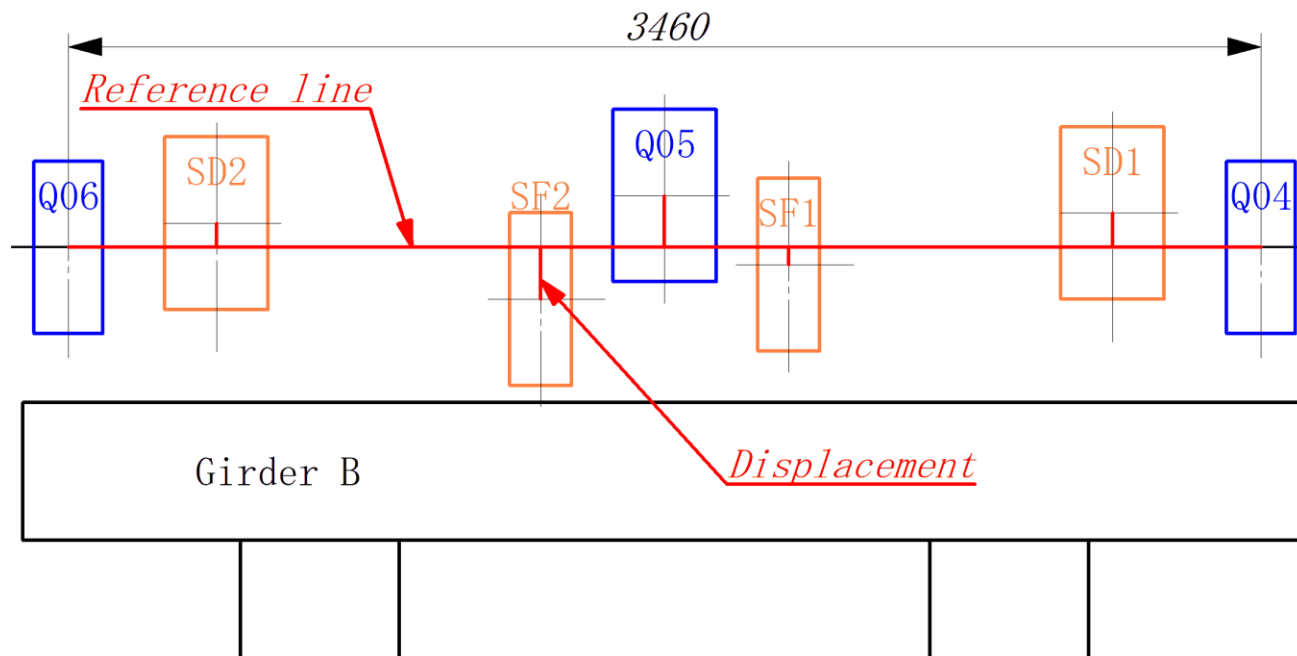
### Reference line :

A straight line passing through two magnetic centers of the both end magnets.

### Displacement :

A distance between each magnet and the reference line.

**Magnetic center of each magnet must be aligned to the reference line.**



## 2. VW Technique (Magnetic Center for Quadrupole)

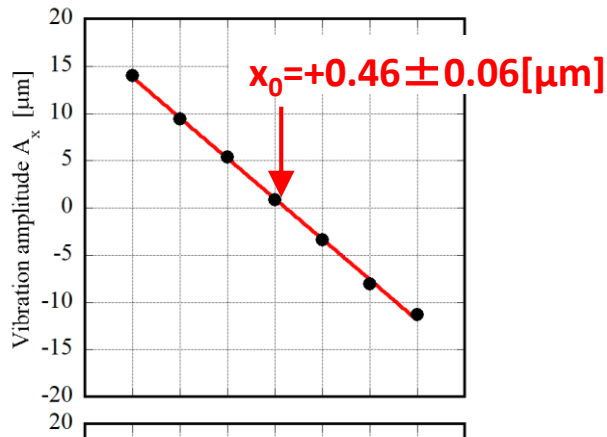
### Magnetic Center in Quadrupole Magnet.

$$B_x(y) = G_q(y - y_0),$$

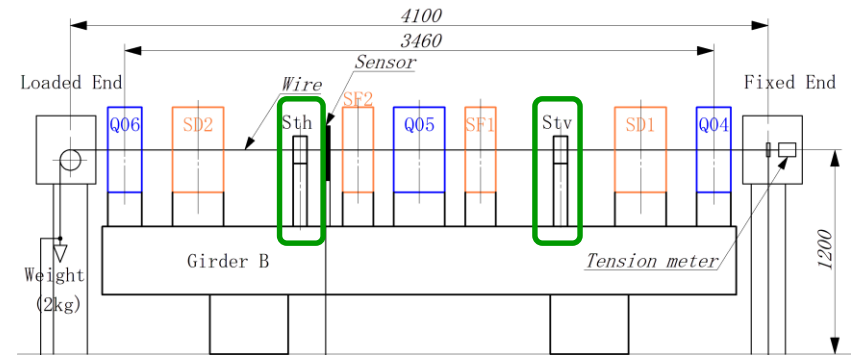
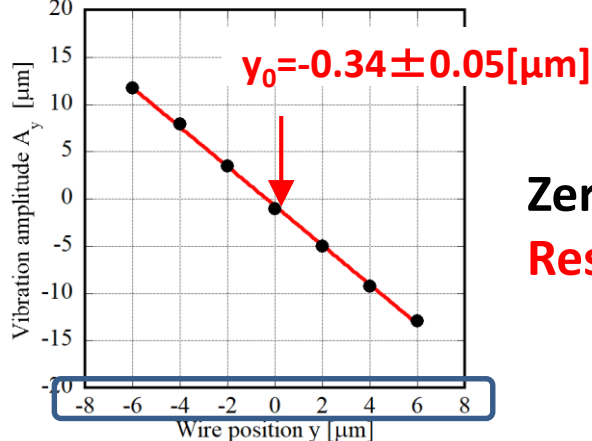
$$B_y(x) = G_q(x - x_0)$$

- Background vibration due to an external field was canceled by *Sth* and *Stv*.
- Only alignment target magnet was excited.
- To obtain the centers,  $x_0$  and  $y_0$ , the wire was scanned in  $y$  and  $x$ , respectively.

Q04  
 $B_y$  vs.  $x$



Q04  
 $B_x$  vs.  $y$



Zero amplitude indicates the magnetic center.  
**Resolution < 0.1 [ $\mu\text{m}$ ]**



## 2. VW Technique (Magnetic Center for Sextupole)

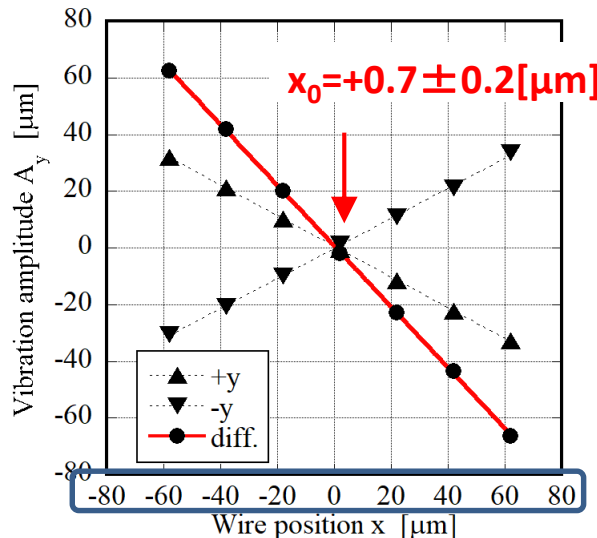
### Magnetic Center in Sextupole Magnet.

$$B_x(x, y) = G_s(x - x_0)(y - y_0),$$

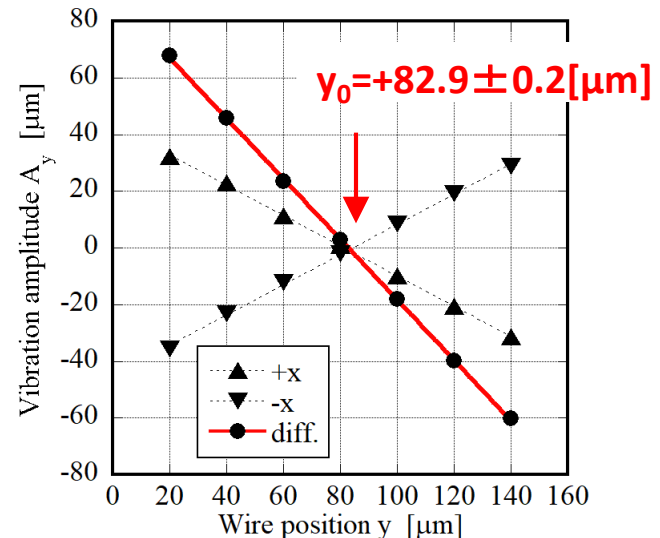
$$B_y(x, y) = \frac{1}{2} G_s [(x - x_0)^2 - (y - y_0)^2]$$

- The  $B_x$  component was chosen for measuring both  $x$  and  $y$  directions.
- Only alignment target magnet was excited.
- The wire was scanned in  $x$  at two vertical offset points.
- To obtain  $x_0$ , an amplitude difference between two offsets was calculated.
- The wire was scanned in  $y$  at two horizontal offset points.
- To obtain  $y_0$ , an amplitude difference between two offsets was calculated.

SD1  
 $B_x$  vs.  $x$



SD1  
 $B_x$  vs.  $y$



Zero amplitude difference indicates the magnetic center. **Resolution < 0.3 [ $\mu\text{m}$ ]**

## 2-1. Wire Sag (Theory)

### Sag distribution in longitudinal direction, $S(s)$

$$S(s) = \alpha \left[ \cosh\left(\frac{s}{\alpha}\right) - \cosh\left(\frac{L}{2\alpha}\right) \right] \cong \frac{1}{8\alpha} (4s^2 - L^2), \quad \alpha \equiv \frac{T}{\rho}.$$

T : Tension [kgf],  $\rho$  : Wire density [kgf/m], L : Wire length [m]  
s : Longitudinal position [m] (s=0 at the center of the wire)

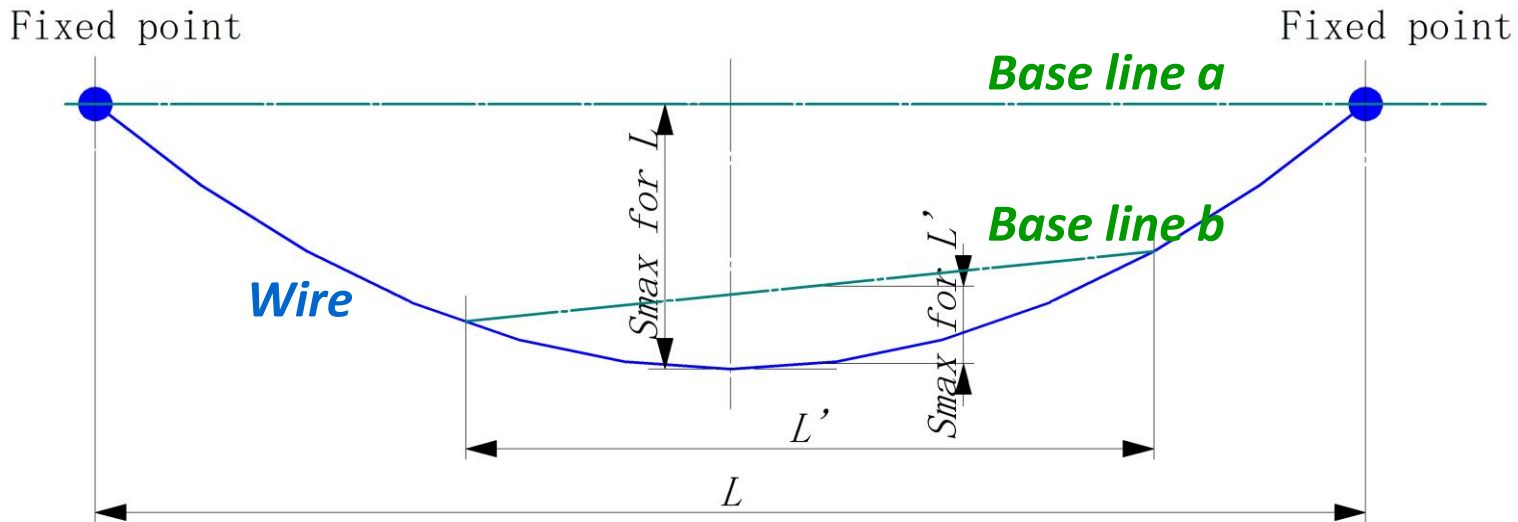
### Maximum Sag, $S_{\max}$

$$S_{\max} = \frac{\rho}{8T} L^2, \quad \left( S_{\max} = \frac{g}{32f_1^2} \right).$$

$f_1$  : Fundamental resonance frequency [Hz]  
g : Acceleration due to gravity [m/s<sup>2</sup>]

## 2-1. Wire Sag (Theory)

$$S_{\max} = \frac{g}{32f_1^2} \quad (1), \quad S_{\max} = \frac{\rho}{8T} L'^2 \quad (2).$$



- Eq. (1) gives the maximum sag for the full wire length  $L$ , including fixed points. (The sag for the length  $L$  is defined as a displacement from the “**Base line a**”.)
- Eq. (2) gives the maximum sag for any partial section  $L'$  in the length  $L$ . (The sag for the length  $L'$  is defined as a displacement from the “**Base line b**”.)

**In case of the latter, we can choose any section in the length  $L$ .**

## 2-1. Wire Sag (Theory)

### Sag distribution in longitudinal direction, $S(s)$

$$S(s) = \alpha \left[ \cosh\left(\frac{s}{\alpha}\right) - \cosh\left(\frac{L}{2\alpha}\right) \right] \cong \frac{1}{8\alpha} (4s^2 - L^2), \quad \alpha \equiv \frac{T}{\rho}.$$

T : Tension [kgf],  $\rho$  : Wire density [kgf/m], L : Wire length [m]  
s : Longitudinal position [m] (s=0 at the center of the wire)

### Maximum Sag, $S_{\max}$

$$S_{\max} = \frac{\rho}{8T} L^2, \quad \left( S_{\max} = \frac{g}{32f_1^2} \right). \quad \begin{array}{l} f_1 : \text{Fundamental resonance frequency [Hz]} \\ g : \text{Acceleration due to gravity [m/s}^2\text{]} \end{array}$$

$S_{\max}$  (Q04-Q06) = 198 [ $\mu\text{m}$ ] (Not negligibly small)

Using a sag-observation bench, we measured sag full profile at the same tension.

1. Maximum sag was evaluated, and was compared with the theoretical value.
2. Local kinks were observed to choose a suitable wire.

## 2-1. Wire Sag (Theory)

### Sag distribution in longitudinal direction, $S(s)$

$$S(s) = \alpha \left[ \cosh\left(\frac{s}{\alpha}\right) - \cosh\left(\frac{L}{2\alpha}\right) \right] \cong \frac{1}{8\alpha} (4s^2 - L^2), \quad \alpha \equiv \frac{T}{\rho}$$

T : Tension [kgf],  $\rho$  : Wire density [kgf/m], L : Wire length [m]  
 s : Longitudinal position [m] (s=0 at the center of the wire)

### Maximum Sag, $S_{\max}$

$$S_{\max} = \frac{\rho}{8T} L^2, \quad \left( S_{\max} = \frac{g}{32f_1^2} \right), \quad \begin{array}{l} f_1 : \text{Fundamental resonance frequency [Hz]} \\ g : \text{Acceleration due to gravity [m/s}^2\text{]} \end{array}$$

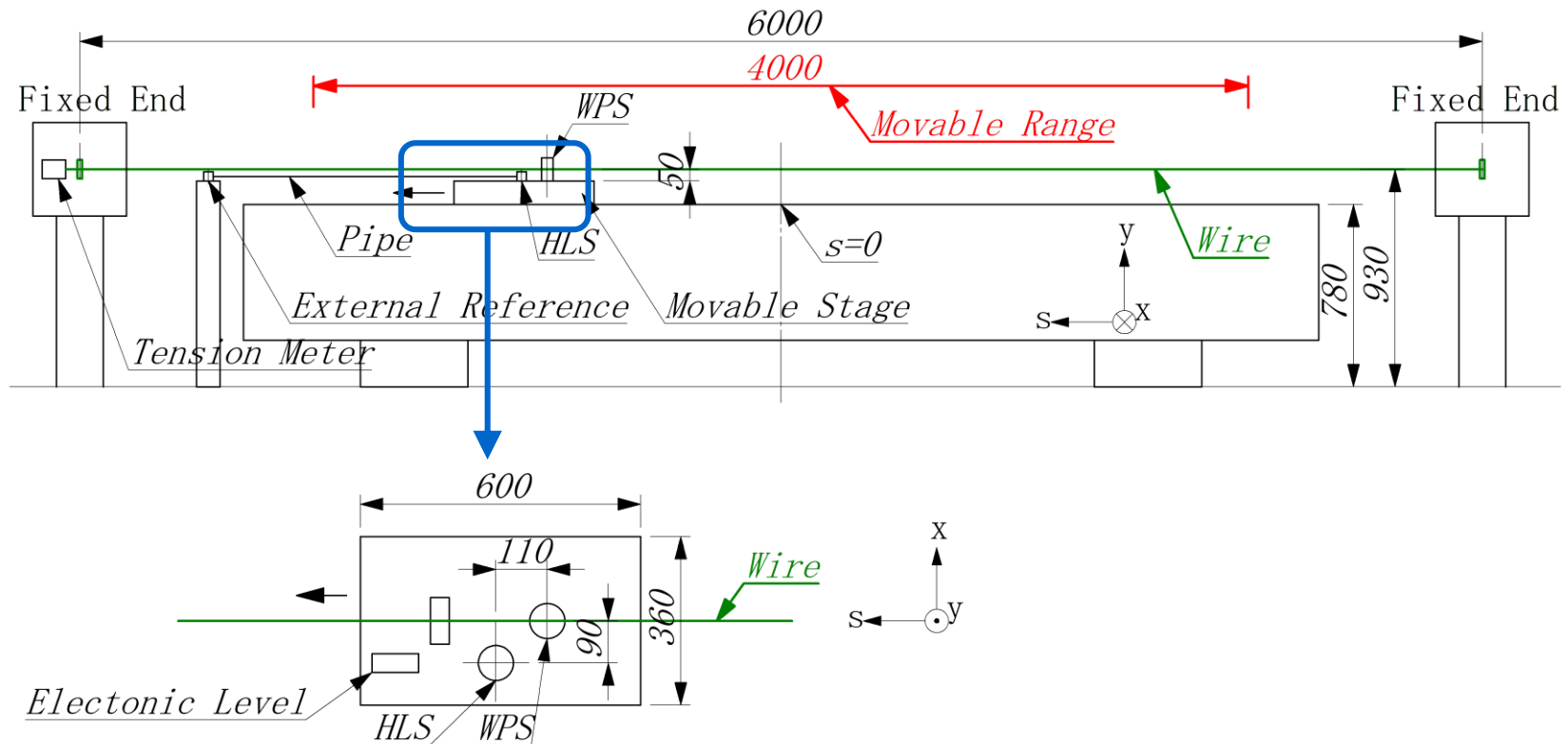
**We chose the equation.**

$S_{\max}$  (Q04-Q06) = 198 [ $\mu\text{m}$ ] (Not negligibly small)

Using a sag-observation bench, we measured sag full profile at the same tension.

1. Maximum sag was evaluated, and was compared with the theoretical value.
2. Local kinks were observed to choose a suitable wire.

## 2-1. Wire Sag (Sag Observation Bench)



- A 6-m long Be-Cu wire (0.2mm-dia.) was stretched above a movable stage. (Tension = 2 kgf, the same tension for the on-girder alignment setup)
- To measure wire height distribution, a WPS sensor was placed on the stage.
- We moved the stage automatically along s-axis in “the movable range”.
- To correct vertical deviations from straightness, two HLS sensors were placed.

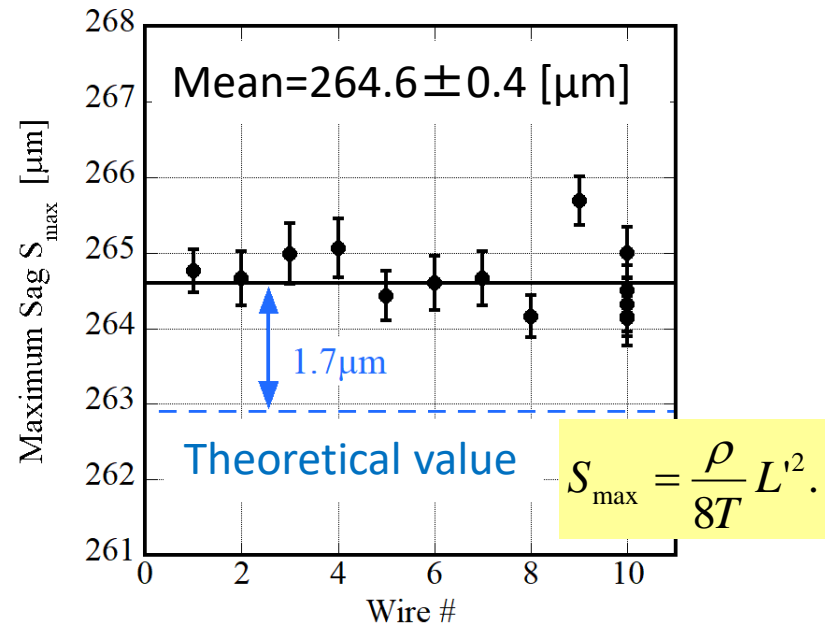
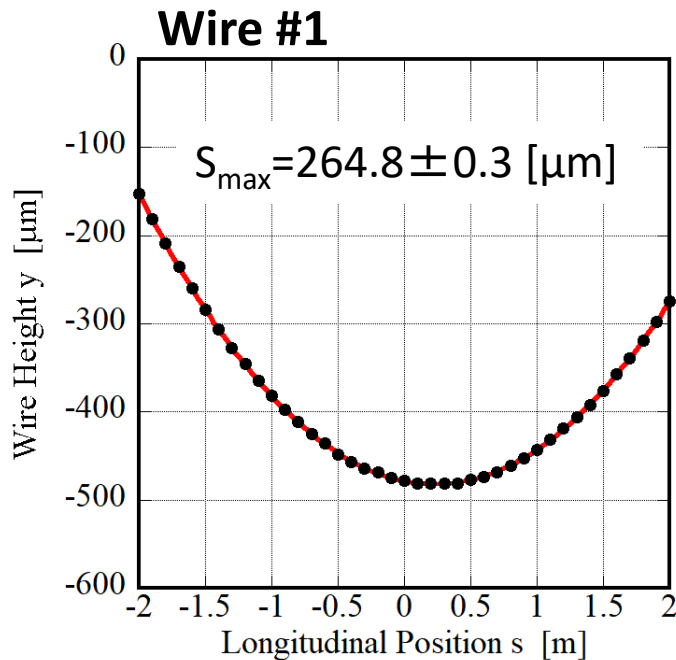
## 2-1. Wire Sag (Maximum Sag of Actual Wires)

The wire height distributions were measured for 10 actual wires (in 100mm step), and were fitted to the following function.

$$y(s) = as^2 + b + cs.$$

$as^2$  : Sag-term [m]

$b+cs$  : Height offsets of the wire ends [m]

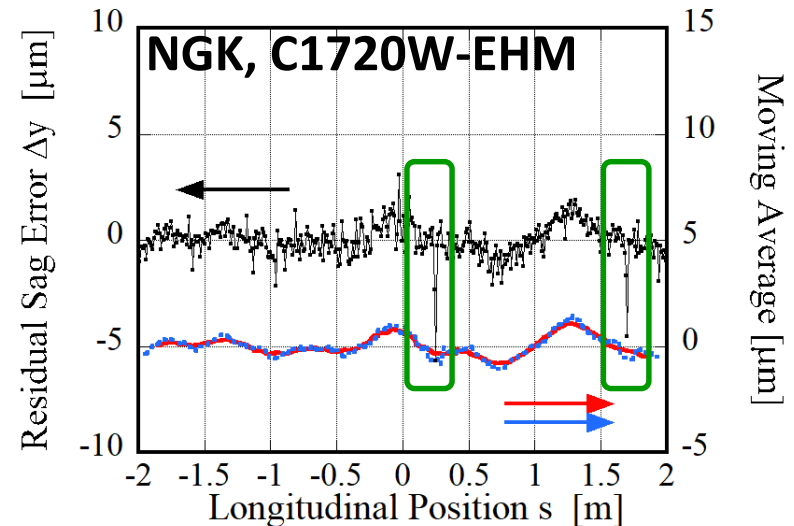
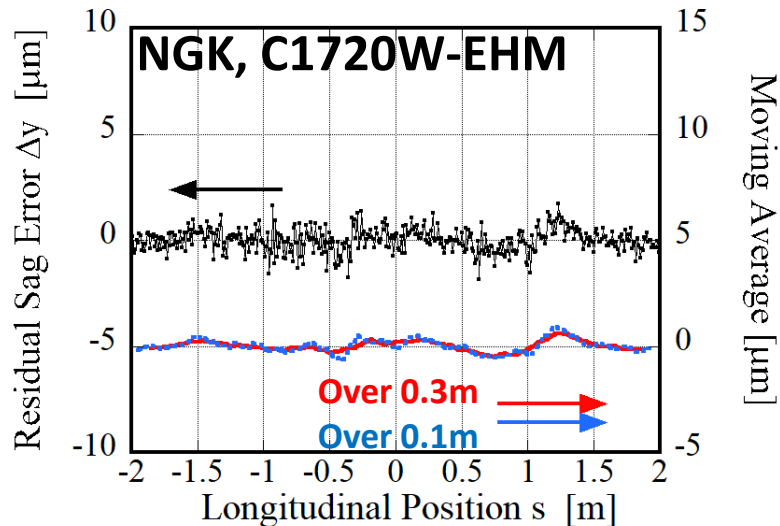


- Difference between mean value and the theoretical one exceeds one S.T.D.
- However, the difference is much smaller than the alignment tolerance.

## 2-1. Wire Sag (Local Kinks of Actual Wires)

The wire height distributions were measured for 10 actual wires (in 10mm step).  
 “A residual sag error” was defined.

$$\Delta y(s) \equiv y(s)_{\text{measured}} - y(s)_{\text{fitted}}.$$



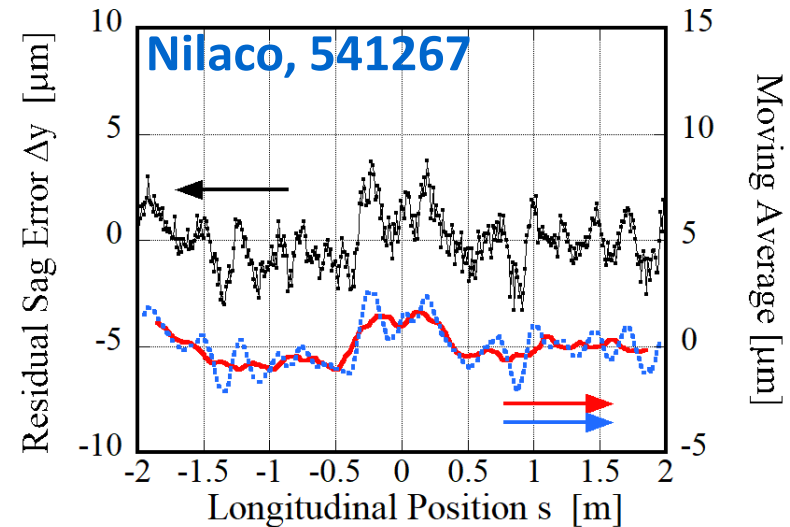
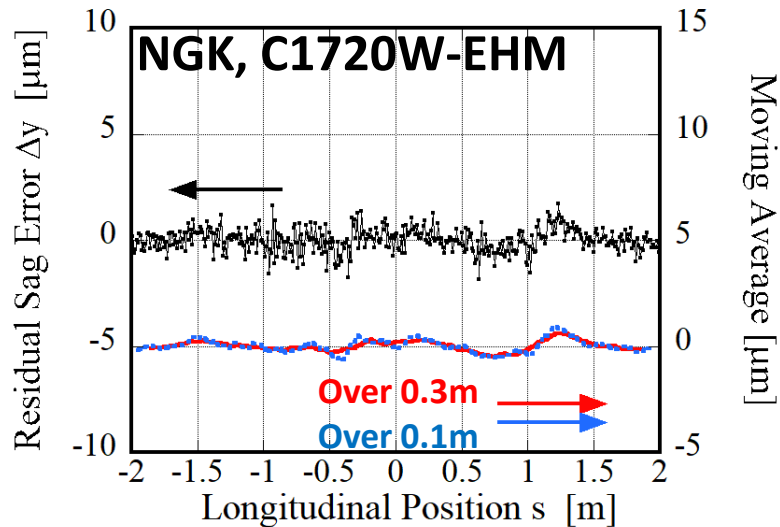
- Local kink was observed in 4 wires. Total number of kinks was 7.
- The maximum error was 5  $\mu\text{m}$ . The maximum width was 30 mm.
- The kink is averaged over the length of alignment target magnet.

\* We cannot discuss within  $\pm 2 \mu\text{m}$   
 because a fluctuation in the ambient air temperature was 0.23 K during one scan (4 hr).



## 2-1. Wire Sag (Local Kinks of Actual Wires)

“The residual sag error” was observed for another type wire (in 10mm step).  
Test wire : Nilaco Ltd., 541267 (No heat-treated)



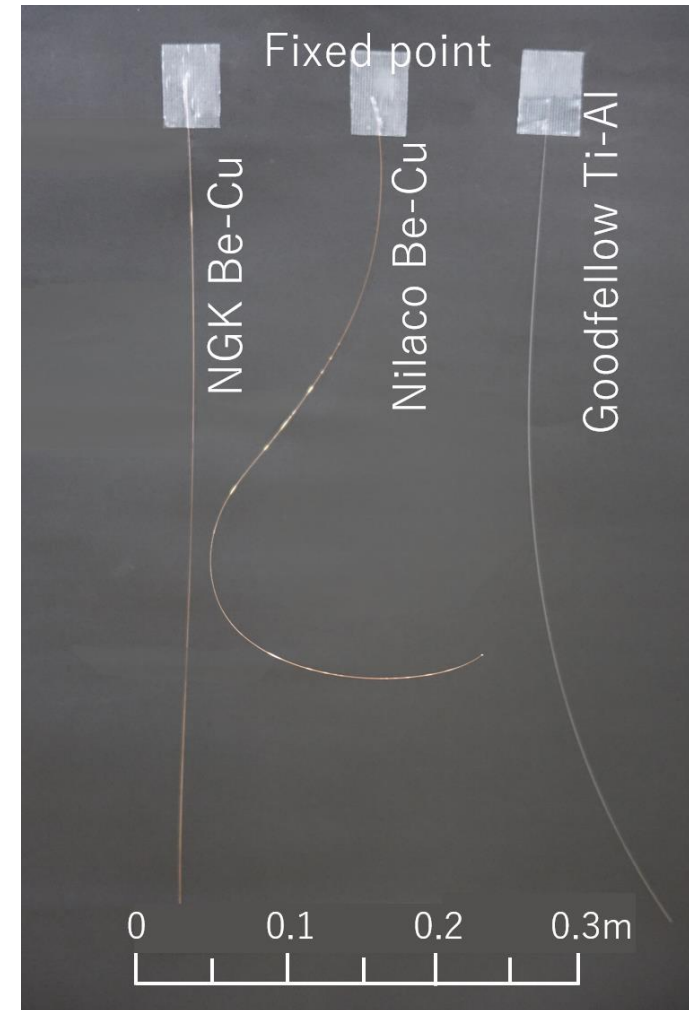
- For Nilaco wire, “the residual sag error” was observed to be periodic.
- The maximum error was 4 μm. The period was 250 mm.
- The error is not suppressed effectively by the moving average.

## 2-1. Wire Sag (Compare the Straightness)

- The **NGK wire** and **Nilaco wire** were fixed at their top ends.
- These wires were allowed to hang down without any force.
- The **Nilaco wire** retained the curve of the original winding for shipping.
- The straightness of the NGK wire is clearly superior to that of Nilaco wire.

This is why

we chose the “NGK C1720W-EHM wire”.



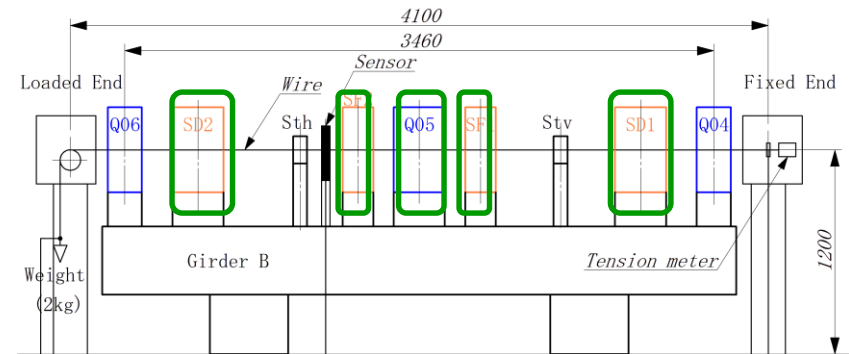
## 2-2. Demonstration of On-Girder Alignment

### (1) Pre-alignment

- Positions of magnets on the *Girder B* were pre-aligned using a laser tracker.
- Mechanical centers of these magnets were adjusted to within 0.1 mm.
- Yaw, pitch, and roll angles were corrected to within 0.1 mrad.

### (2) On-girder alignment was demonstrated by the VW Technique.

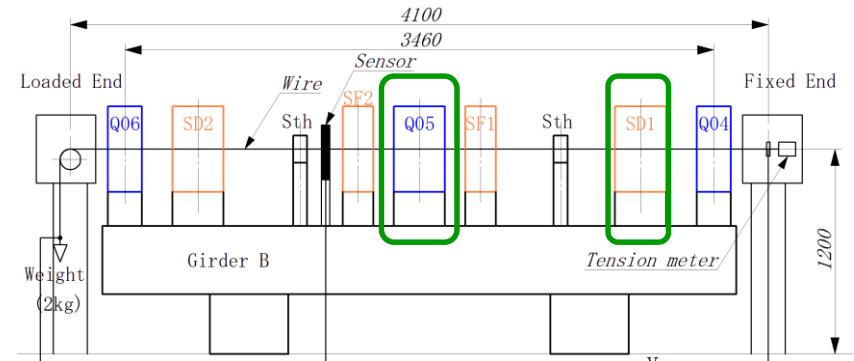
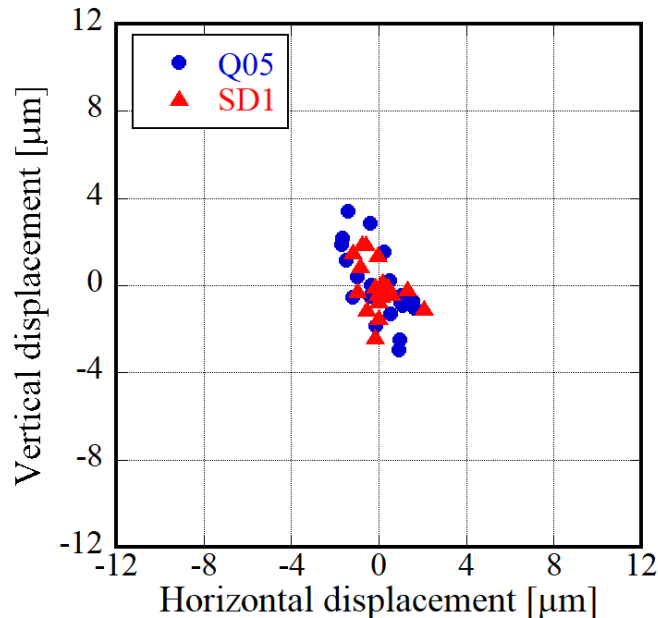
Magnet	Remaining Displacement (x, y) [ $\mu\text{m}$ ]
Q04	-
SD1	(0.0, +0.8)
SF1	(-7.8, -3.3)
Q05	(-4.4, 0.0)
SF2	(+4.2, -2.2)
SD2	(-5.2, 3.5)
Q06	-



With a conventional position adjustment mechanism, the displacements was suppressed with sufficient precision.

## 2-3. Overall Random Error

- The displacements of **Q05** and **SD1** on the **Girder B** were repeatedly measured 20 times both before and after the following handling processes.
  - I. Released the tension once, and then re-tensioned again : 5 times
  - II. Removed the wire once, and then re-tensioned the same wire : 10 times
  - III. Re-installed new wire : 4 times

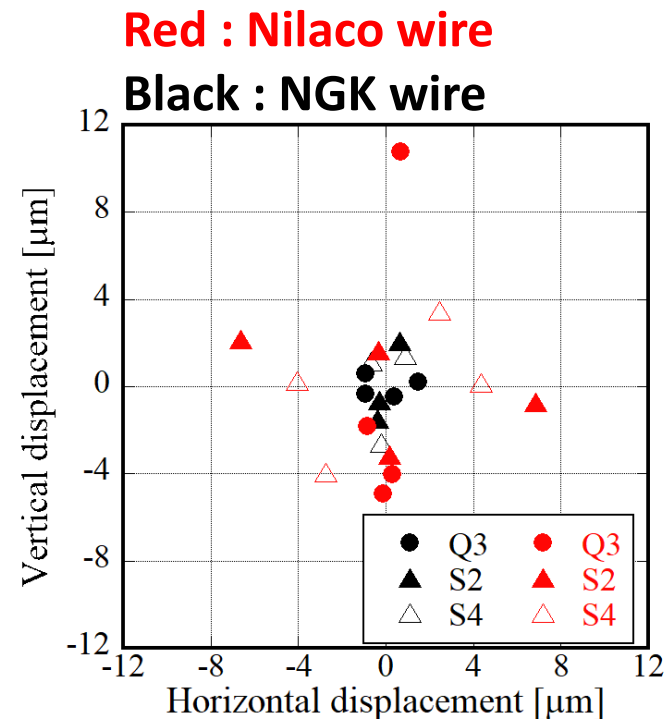
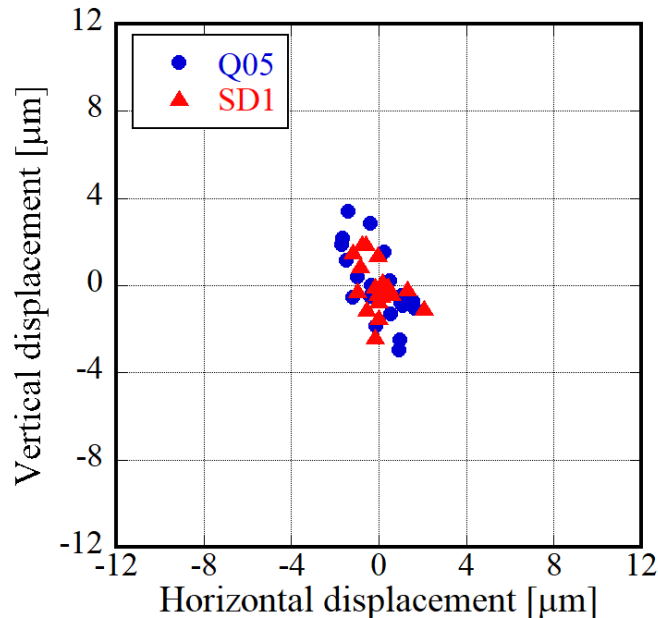


**Thanks to choosing a suitable wire,**  
**standard deviation is 1.7 [μm] even in the worst case !**

## 2-3. Overall Random Error

If the Nilaco wire is used, the overall random error became larger.

- Using the present ring magnets, the overall random error was observed for the Nilaco wire and NGK wire.



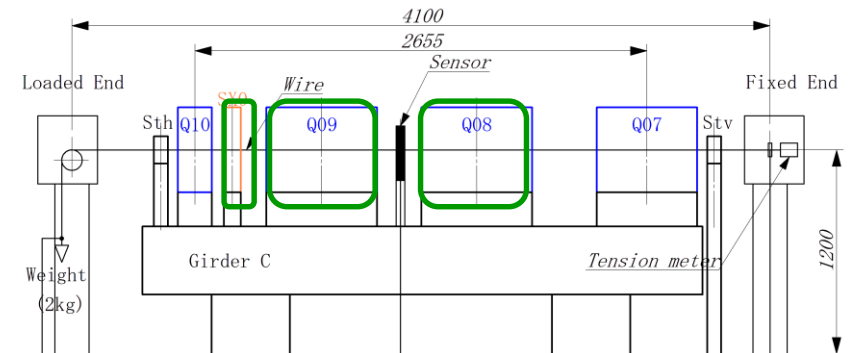
For the Nilaco wire,

standard deviation is 7.3 [ $\mu\text{m}$ ] in the worst case !

## 2-4. Change in the Magnetic Center (Transport)

- After on-girder alignment, the *Girder C* was moved to another room by a truck.
- Pitch and roll of the girder was corrected.
- The reference line was re-defined, and the displacements were observed.

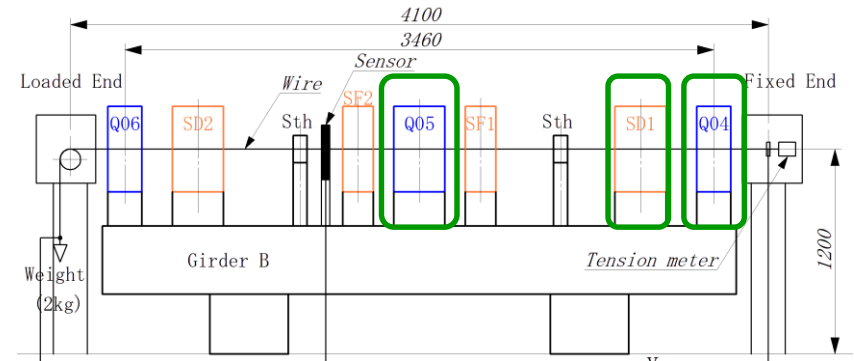
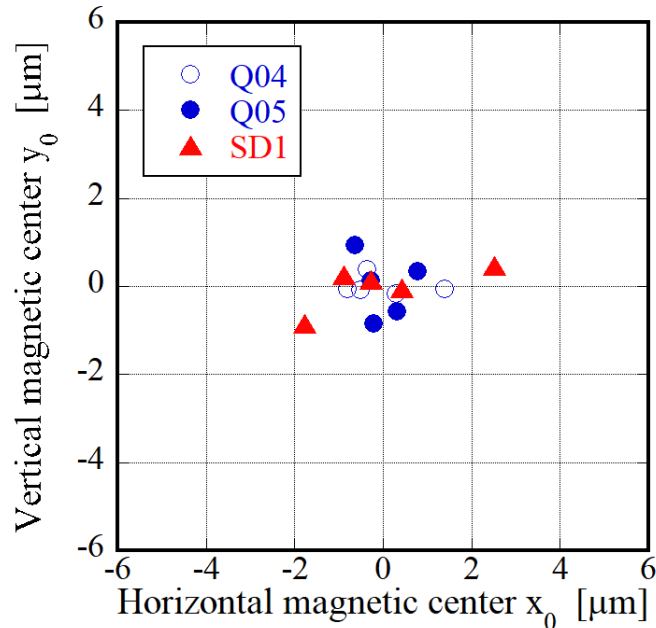
Magnet	Change in the Displacement (x, y) [ $\mu\text{m}$ ]
Q07	-
Q08	(+8, -3)
Q09	(+7, +4)
SX0	(-3, -3)
Q10	-



**The change was less than the alignment tolerance.**  
**However, the change exceeds the overall random error.**

## 2-4. Change in the Magnetic Center (Reassembly)

- The magnetic centers of **Q04**, **Q05** and **SD1** on the **Girder B** were measured both before and after the reassembly of the magnet core.
- Reassembly was repeated **4 times**.



The change was much smaller than the alignment tolerance.

## 2-5. Fiducialization

### I. Purpose

- For the girder-to-girder alignment, the reference line must be transferred to fiducial point on the top of the magnets.

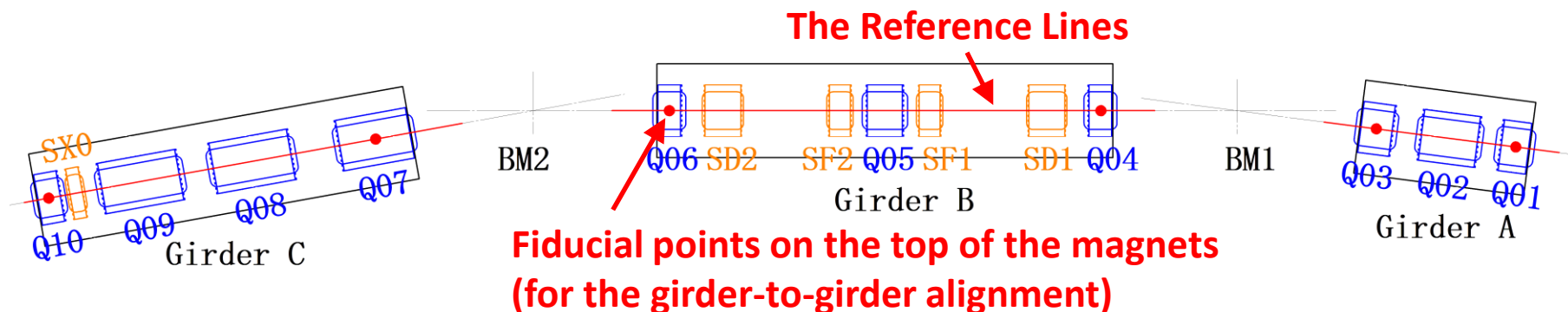
### II. Our Proposal

- Direct measurement of the reference line using a laser tracker.

### III. Method

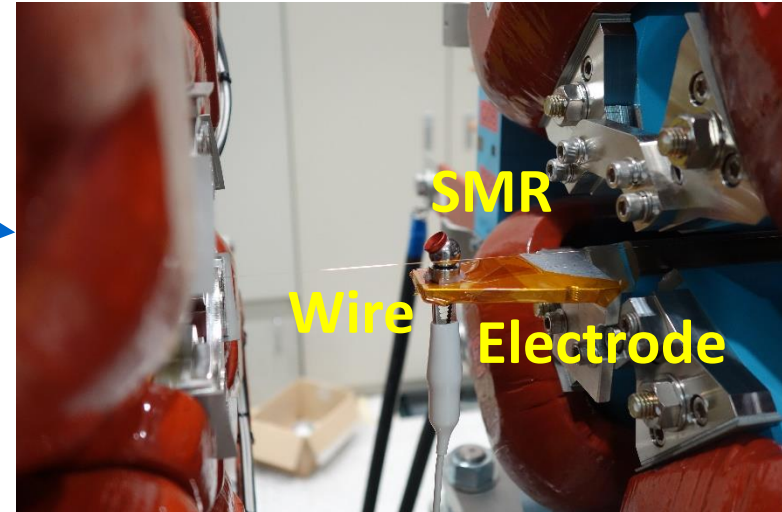
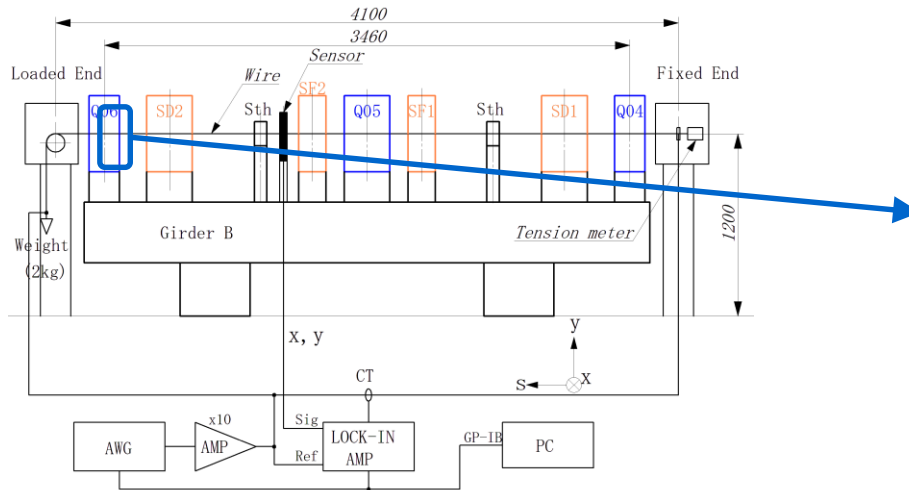
- SMR targets are attached near the center of QMs placed at the both ends.
- Contact points (Wire-SMR) are measured by watching electric resistance.
- The SMR center is estimated by a least-squares fit with a circle function.

We tested the method using the *Girder B* and *Q06*.





## 2-5. Fiducialization



A 0.5"-SMR was attached at Q06.

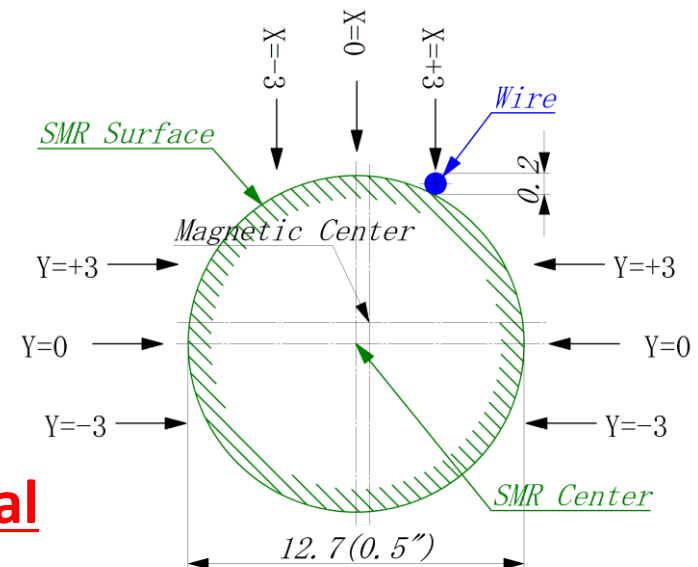
- The wire was brought closer to the SMR using x-y stage with 1- $\mu\text{m}$  step until resistance changed to a finite value.
- Contact points were recorded at 9 points.

### Result of Estimated SMR Center Position :

S. T. D. of the fit : 0.6 $\mu\text{m}$ (x), 0.9 $\mu\text{m}$ (y)

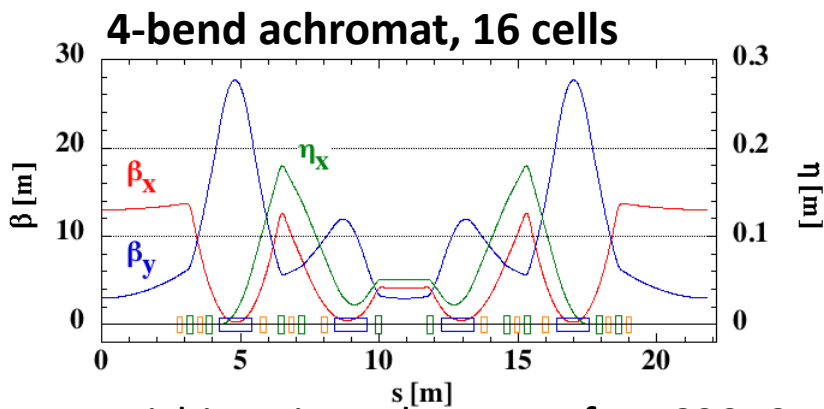
S. T. D. for 10 measurement : 0.7 $\mu\text{m}$ (x), 1.4 $\mu\text{m}$ (y)

Reference line can be transferred to external fiducial point with a laser tracker system.



# Application to a New Ring

## Conceptual Drawing “Highly Brilliant Compact 3 GeV Light Source Project in JAPAN”



N. Nishimori, et al., Proc. of IPAC2019.

	New 3GeV Ring
Energy (GeV)	3
Stored current (mA)	400
Circumference (m)	348.84
Emittance (nmrad)	1.14

**We plan to apply the same alignment scenario for the new ring.**

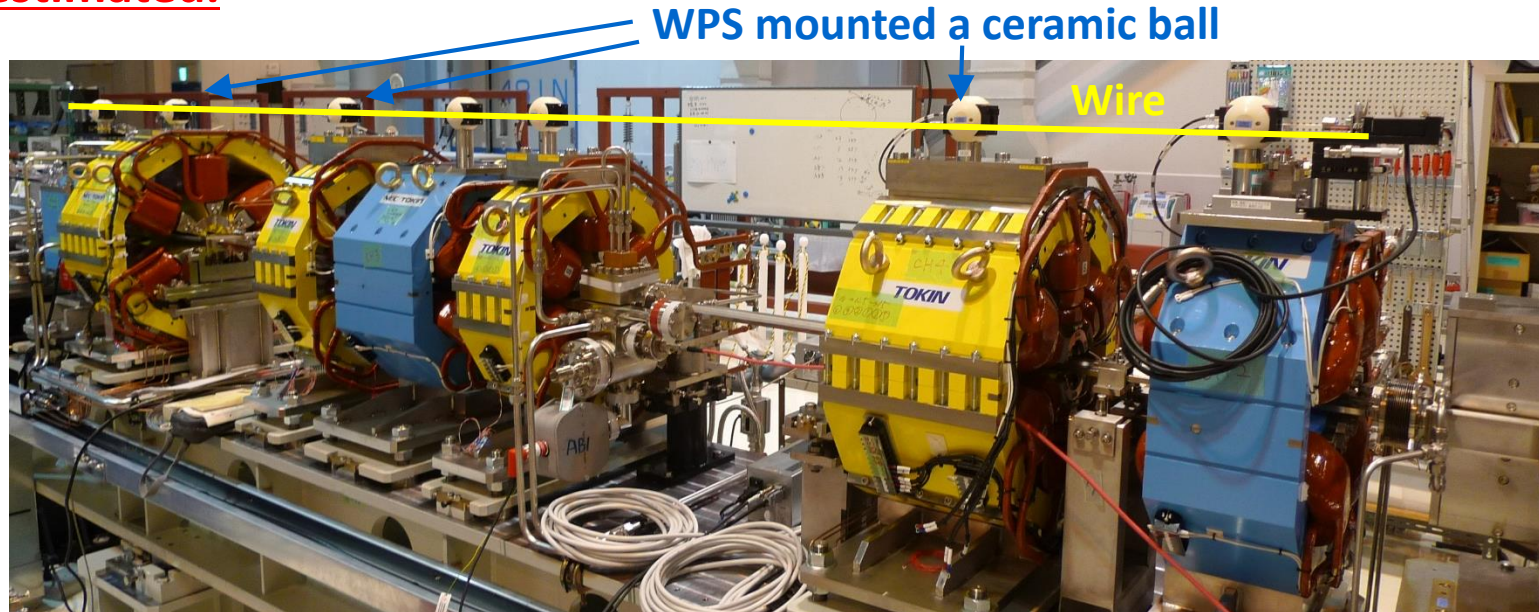
### 3. Summary

- Thanks to choosing a suitable wire, the overall random error was much smaller than the required alignment tolerance.
- We confirmed that the change in the magnetic center due to reassembly was much smaller than the tolerance.
- The change in the magnetic center due to the transport exceeds the overall random error. We plan to repeat the transport tests to figure out the cause of the change.
- In 2022, we will apply the VW Technique and the alignment scenario for the 3 GeV Light Source Project in Japan.

## Appendix (Monitoring of the Magnet Position)

We have developed Wire Alignment Monitoring System (WAMS).

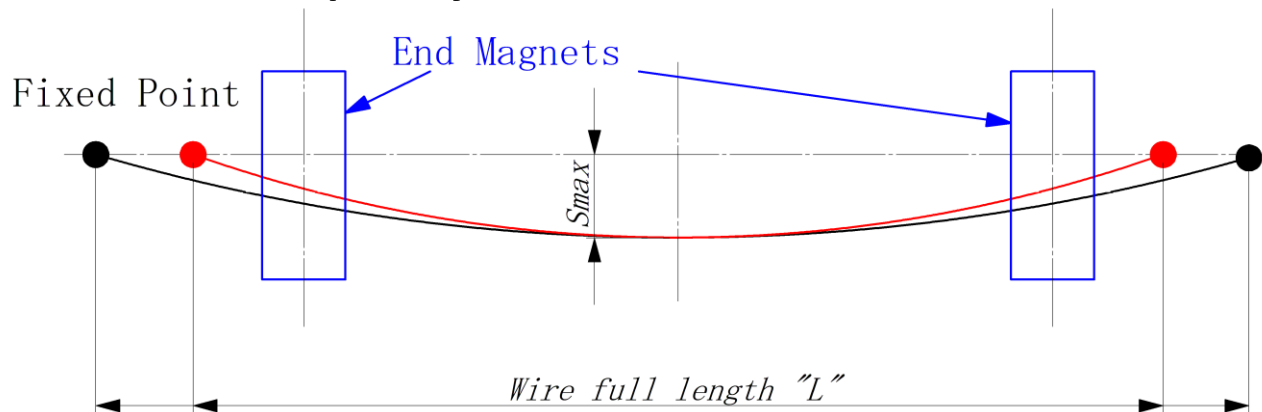
- After installation of vacuum chambers, we cannot install the wire at the bore center. Instead, a wire is tensioned above the magnets.
- The wire is fixed on the both end magnets.
- WPS sensors are placed on the other magnets.
- By measuring the wire position, change in the magnet positions can be estimated.



## Appendix (Two Ways to Define the Theoretical Sag)

$$S_{\max} = \frac{g}{32f_1^2} \quad (1), \quad S_{\max} = \frac{\rho}{8T} L^2 \quad (2).$$

- In case of Eq.(1), the same resonance frequency gives the same sag full profile for the full wire length  $L$  including the fixed points at both wire ends.
- We adopt a ball-bearing pulley to maintain the wire tension. The full wire length  $L$  cannot be well determined because the contact point between the wire and the pulley surface is not identified clearly.
- The sag full profile between the both end magnets cannot be uniquely defined by the resonance frequency.

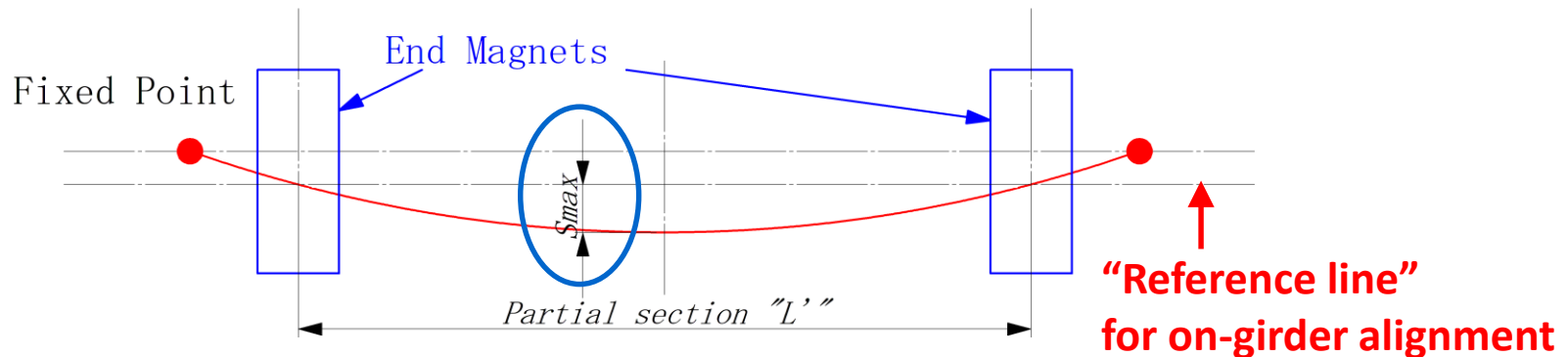


Even if the maximum sag is the same for the  $L$ , the sag full profile is different between the both end magnets.

$$S_{\max} = \frac{g}{32f_1^2} \quad (1),$$

$$S_{\max} = \frac{\rho}{8T} L'^2 \quad (2).$$

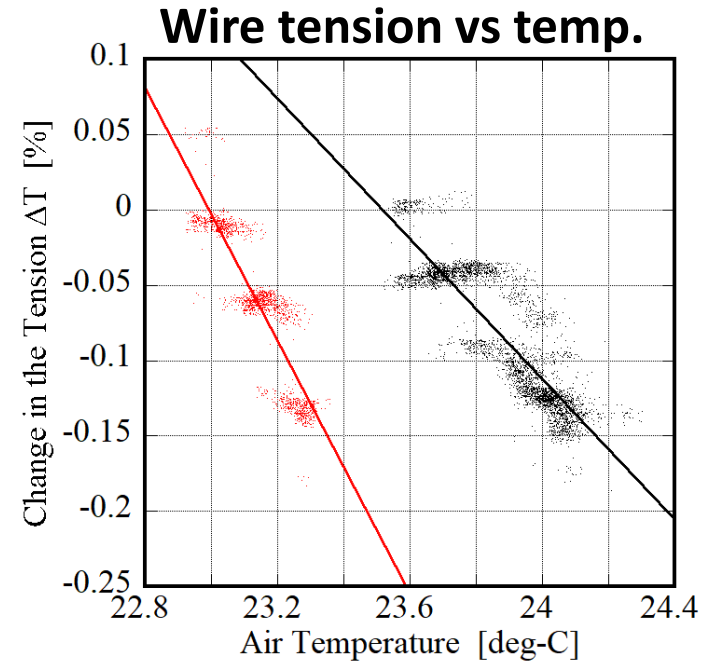
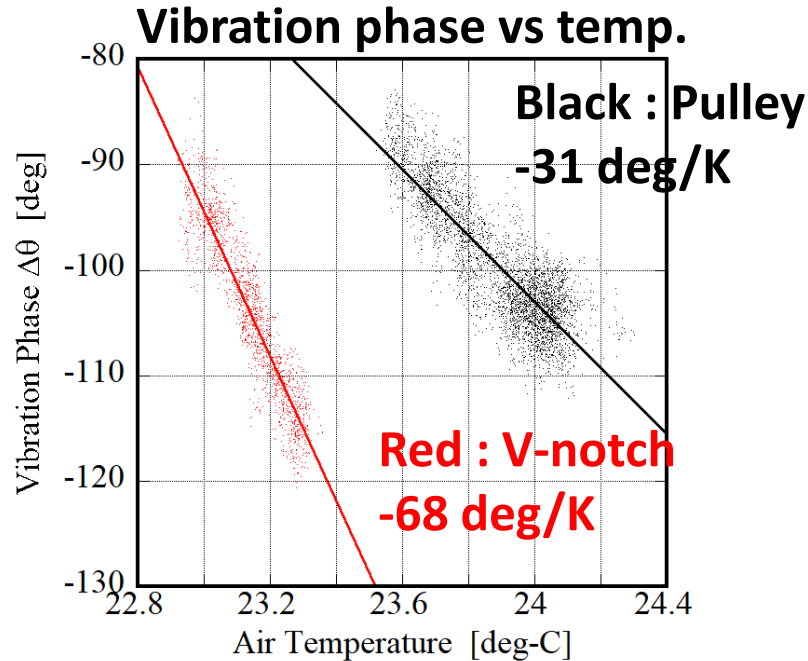
- In case of Eq.(2), the same wire tension and the wire density gives the same sag full profile in any partial section  $L'$ .
- The sag full profile between the both end magnets can be uniquely defined regardless of the condition of the fixed points.



$S_{\max}$  is defined as maximum displacement from the reference line.

The same wire tension and the wire density gives the same sag full profile in  $L'$ .

At the loaded end, we adopted a ball-bearing pulley.



- Vibration phase is equal to +90 (or -90) [deg] at resonance frequency.
- When a V-notch is attached, temperature coefficient of the phase increases.
- A ball-bearing pulley significantly suppresses a fluctuation in the phase and in the tension.

- Horizontal vibration generates a fluctuation in vertical vibration (See Fig.A) because the resonance frequencies in  $x$  and  $y$  did not match perfectly.
- For sextupole magnets, we observed  $B_x$  component at four offset points, where  $B_y$  component is not negligible.
- The additional magnets,  $S_{th}$  and  $S_{tv}$ , helps restraint of the fluctuation.

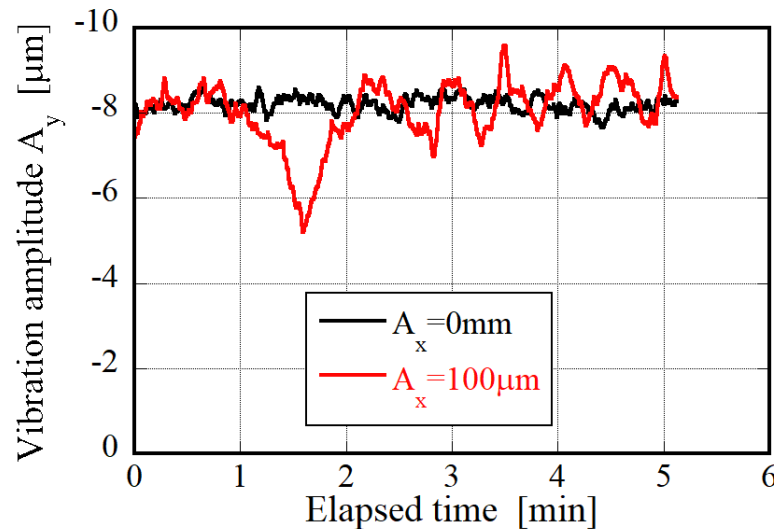


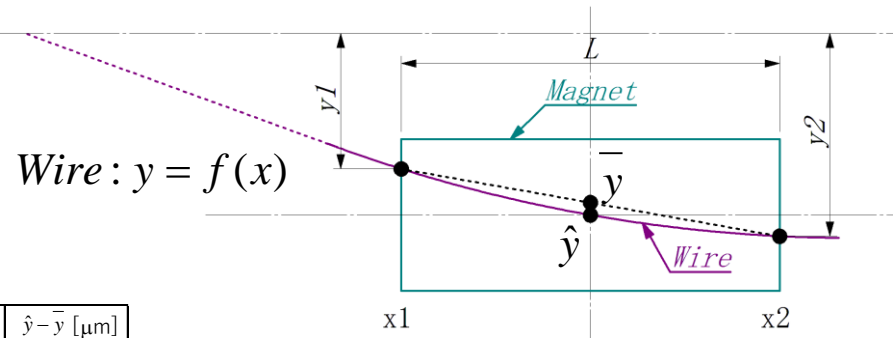
**Figure A** Example of temporal changes in amplitude of vertical vibration.  
**Black** : The amplitude when horizontal vibration was canceled by  $S_{th}$ .  
**Red** : The amplitude when horizontal vibration amplitude was 100  $\mu\text{m}$ .



# Appendix (Mean Sag and Effective Sag)

A difference between “Mean Sag” and “Effective Sag” is not negligible at “Long Magnet”.

We corrected using the Effective Sag”.



Girder	Magnet	L[m]	y1[ $\mu\text{m}$ ]	y2[ $\mu\text{m}$ ]	$\bar{y}$ [ $\mu\text{m}$ ]	$\hat{y}$ [ $\mu\text{m}$ ]	$\hat{y} - \bar{y}$ [ $\mu\text{m}$ ]
A	Q01	0.24	-17.2	-34.7	-25.9	-27.7	-1.7
	Q02	0.47	-42.9	-45.1	-44.0	-46.4	-2.4
	Q03	0.27	-36.4	-17.2	-26.8	-28.8	-2.1
B	Q04	0.20	-42.5	-87.1	-64.8	-67.9	-3.1
	SD1	0.30	-122.8	-173.0	-147.9	-150.5	-2.6
	SF1	0.18	-244.9	-253.3	-249.1	-249.5	-0.4
	Q05	0.30	-256.6	-256.6	-256.6	-257.5	-1.0
	SF2	0.18	-253.3	-244.9	-249.1	-249.5	-0.4
	SD2	0.30	-173.0	-122.8	-147.9	-150.5	-2.6
	Q06	0.20	-87.1	-42.5	-64.8	-67.9	-3.1
C	Q07	0.70	-36.4	-145.2	-90.8	-107.4	-16.6
	Q08	0.70	-170.3	-191.5	-180.9	-186.5	-5.5
	Q09	0.65	-182.8	-123.3	-153.0	-159.8	-6.8
	Q10	0.20	-74.0	-36.4	-55.2	-57.9	-2.7

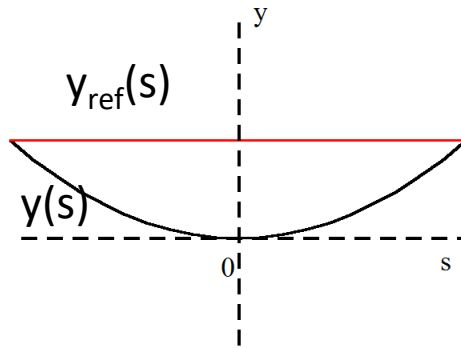
$$\bar{y} = \frac{1}{2}(y_1 + y_2) \quad : \text{Mean Sag}$$

$$\hat{y} = \frac{\int_{x_1}^{x_2} S(x) f(x) dx}{\int_{x_1}^{x_2} S(x) dx} \quad : \text{Effective Sag}$$

$S(x)$  : Vibration Sensitivity

# Appendix (Sag with Offset)

Offset = 0

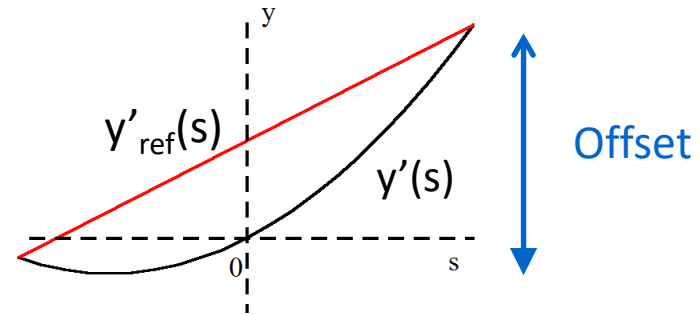


$$y_{ref}(s) = C$$

$$y(s) = a \left\{ \cosh\left(\frac{s}{a}\right) - 1 \right\}$$

$$Sag(s) \equiv y_{ref}(s) - y(s)$$

Offset = h



$$y'_{ref}(s) = \frac{h}{L}s + C'$$

$$y'(s) = a \left\{ \cosh\left(\frac{s+s_0}{a}\right) - \cosh\left(\frac{s_0}{a}\right) \right\}, \quad s_0 = \frac{ah}{L}$$

$$Sag'(s) \equiv y'_{ref}(s) - y'(s)$$

$a = T/\rho$ ,  $T$ : Tension[kgw],  $\rho$ : Wire density[kg/m]  
 $L$ : Wire length(=3.6[m]),  $h$ : Offset

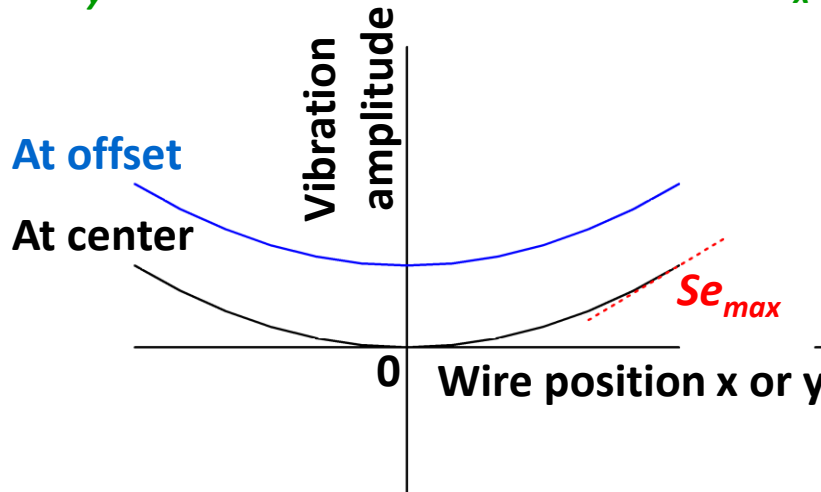
**A difference,  $Sag(s) - Sag'(s) < 2.1 \times 10^{-4} [\mu m]$  (@ $h=5[\text{mm}]$ ) !**

Error Sources	R&D
Resolution of the VW Technique	Unnecessary
Overall Random Error of the VW Technique	Done
Adjustment Mechanism of Magnet position using conventional bolts and nuts mechanism	Unnecessary
Transport of the Common Girder	Survey required
Reassembly of the Magnet using keyway structure at the core joint	Unnecessary
Fiducialization for the Girder-to girder alignment	Done

# Appendix (Why did We Choose the $B_x$ Component)

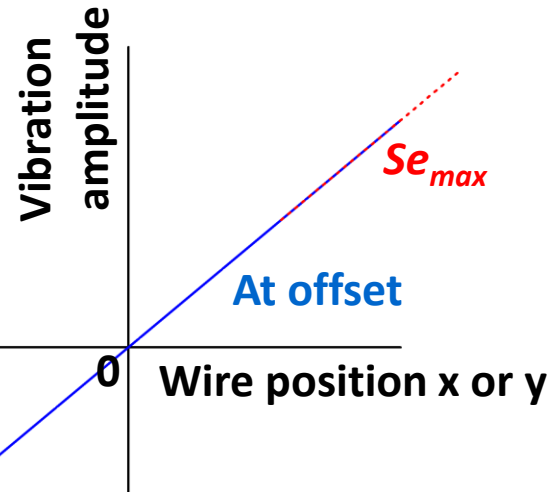
- A maximum sensitivity of the vibration  $Se_{max}$  is defined in the range of wire scan.
- In case of  $B_y$  component,
    - The sensitivity  $Se_{max}$  is the same at offset, and is not adjustable.
  - In case of  $B_x$  component,
    - The sensitivity  $Se_{max}$  depends on an amount of the offset, and is adjustable.
  - The sensitivity of the  $B_x$  is 16 times or more as large as that of  $B_y$  when the wire is placed at 1 [mm].

$B_y$  component



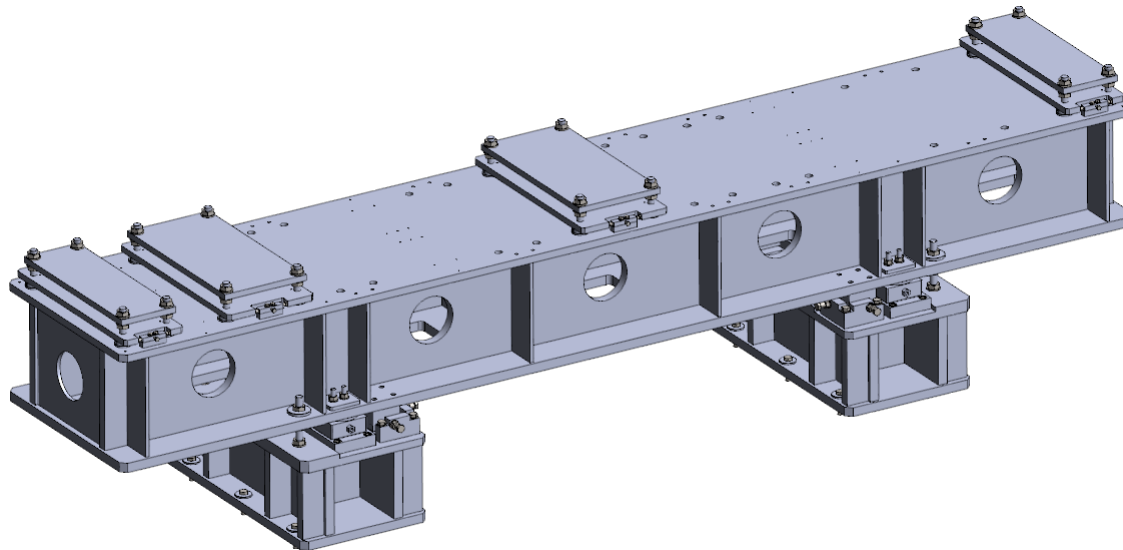
$$(Se_{max})_x \propto \frac{dB_y}{dx} = G_s x, \quad (Se_{max})_y \propto \frac{dB_y}{dy} = G_s y$$

$B_x$  component



$$(Se_{max})_x \propto \frac{dB_x}{dx} = G_s y_{offset}, \quad (Se_{max})_y \propto \frac{dB_x}{dy} = G_s x_{offset}$$

- Four-point support was adopted to suppress a deformation caused by a vertical variation of the floor. to simplify an adjustment process.
- A load deflection  $< 50 \mu\text{m}$ .
- An eigen-frequency  $> 110 \text{ Hz}$



Outline of the *Girder B*.

## Appendix (Temperature Dependences)

### Frequency:

Temperature coefficient : -0.02 [Hz/K], -0.071 [%/K]

### Sag:

From the coefficient of the frequency,

Change in the max. sag : 0.56 [ $\mu\text{m}/\text{K}$ ] (negligibly small)

$$S_{\max} = \frac{g}{32f_1^2} \quad \therefore \frac{\Delta S_{\max}}{S_{\max}} = -2 \frac{\Delta f_1}{f_1}$$

### Tension:

From the coefficient of the frequency,

Change in the tension : -0.14 [%/K], -2.8 [gw/K]

$$f_1 = \frac{1}{2L} \sqrt{\frac{T}{\rho}} \quad \therefore \frac{\Delta T}{T} = 2 \frac{\Delta f_1}{f_1}$$

### Wire density:

From the coefficient of the frequency,

Change in the wire density : 0.14 [%/K] (inconsistent)

$$f_1 = \frac{1}{2L} \sqrt{\frac{T}{\rho}} \quad \therefore \frac{\Delta \rho}{\rho} = -2 \frac{\Delta f_1}{f_1}$$